JOURNAL OF CATALYSIS 142, 465–489 (1993)

Cracking Selectivity Patterns in the Presence of Chain Mechanisms. The Cracking of 2-Methylpentane

YINGXIAN ZHAO, G. R. BAMWENDA, AND B. W. WOJCIECHOWSKI[1]

Department of Chemical Engineering, Queen's University, Kingston, Ontario, Canada K7L 3N6

Received October 6, 1992; revised December 22, 1992

Catalytic cracking of 2-methylpentane on HY has been studied at 400, 450, and 500°C and a chain reaction mechanism is used to interpret the selectivity of the reaction. The results of a quantitative description of this mechanism show that protolysis of bonds in the feed molecule at 400°C follows the order

$$(C_t\text{–}C_s) > (C_s\text{–}C_s) > (C_t\text{–}C_p \text{ or } C_s\text{–}C_p) > (C_t\text{–H})$$

in the ratio 0.510/0.416/0.054/0.020, but at 500°C the order becomes

$$(C_t\text{–}C_s) > (C_s\text{–}C_s) > (C_t\text{–H}) > (C_t\text{–}C_p \text{ or } C_s\text{–}C_p)$$

in the ratio 0.625/0.212/0.138/0.025, where p, s, and t refer to primary, secondary, and tertiary carbons. The average reaction chain length is found to be 3.34 at 400°C with isomerization as the dominant reaction in the chain process. The chain length decreases with increasing reaction temperature. This leads to a pronounced decrease in the formation of isomeric products and an increase in the production of C_1–C_5 paraffins and C_2–C_5 olefins. β-Cracking of a parent carbenium ion is very small at 400°C, but becomes noticeable at 500°C. The isomerization process consisting of a skeletal rearrangement of the $C_6H_{13}S^+$ ion and a subsequent abstraction of hydride from a feed molecule in the gas phase dominates conversion at lower temperatures. At higher temperatures, however, the appearance of β-cracking of the C_6^+ ion and the enhancement of the desorption of parent carbenium ions inhibit isomerization. Molecular hydrogen is initially formed from both the protolysis of a C–H bond in the feed molecule and from the formation of coke. The initial molar probability of coke formation is only 0.010 at 400°C, while the H/C ratio in the initial coke is 1.96, substantially below the 2.33 ratio present in the feed. Rising temperature results in an increase in the production of hydrogen and the formation of a more hydrogenated coke.

INTRODUCTION

The mechanism of paraffin cracking is still under vigorous debate (*1–18*). There is no longer any doubt that surface reactions involving carbenium ions play a role in the process (*8, 12, 17*). The question which is not settled is the origin of the first ions in paraffin cracking, i.e., the initiation of the cracking reaction. Some authors have proposed that the cracking is initiated on Lewis sites on zeolite catalysts (*7*), but most now believe that cracking is initiated via the direct protolysis of C–C and/or C–H bonds in the paraffinic feed molecule (*8–19*).

Isomerization of the feed paraffin generally takes place at the same time as cracking. In some cases, the isomerization to cracking ratio is quite large, especially when reaction temperature is low. This relationship between isomerization and cracking needs careful reexamination as it holds clues to the mechanism of all "cracking" processes. Picket *et al.* (*20*) and Tung and McInich (*21*), for example, have suggested that cracking and isomerization of paraffins may proceed via two parallel pathways. We feel, however, that isomerization takes place via the rearrangement of carbenium ions, the same

[1] To whom correspondence should be addressed.

0021-9517/93 $5.00

ions which can take part in any of the other paths followed by such intermediates. The question is therefore how the parent carbenium ion necessary for the isomerization of the feed is formed.

In this work, 2-methylpentane, which has primary, secondary, and tertiary carbon atoms, was chosen as the feedstock and reacted on HY zeolite at temperatures ranging from 400 to 500°C. We use the experimental data obtained at 400°C to formulate the selectivity behaviour of the reaction and, further to a previous discussion of the kinetics of this reaction (*22*), we present a more detailed discussion of the chain mechanism, a comparison of various C–C bond protolysis probabilities, the probabilities of the reaction proceeding down various reaction pathways, and a method for calculating reaction chain lengths. Next we have expanded the investigation using a different apparatus (and a different operator) at 400, 450, 500°C and discuss the influence of temperature on selectivity in terms of reaction path probabilities obtained by using the chain mechanism postulate.

THEORY

Selectivity data forms the basis of our examination of the reaction mechanism. An effective methodology for determining the initial selectivity of products from experimental product yields and conversion data has been defined previously (*23*). For each reaction product, the time-averaged yield sampled from $t = 0$ to t_f is plotted against the average conversion of feed, $\bar{X}$. Each of the plots is enveloped by a single curve, the optimum performance envelop (OPE), which describes the selectivity behaviour of that product as catalyst decay approaches zero. A product is considered primary if the slope at the origin of such a curve is nonzero and secondary if the slope is zero. Primary products are those which are formed directly from the feed molecule without any detectable gas-phase intermediate. A detailed description of what constitutes a primary product according to this methodology has been given previously (*24*).

EXPERIMENTAL

2-Methylpentane of 99 + % purity was obtained from Aldrich and used without further purification. The main impurity was 3-methylpentane (0.55%).

HY zeolite was prepared from NaY (BDH CHEM., Lot. no. 45912, 13Y) by repeated exchange with 0.5 *M* NH_4NO_3 solution at 20°C for 24 h. Between exchanges, the catalyst was dried at 110°C for 24 h, then calcinated in air at 500°C for 2 h. After 10 such exchanges, the catalyst was steamed at 200°C for 2 h. The powder was pelletized, crushed, and sieved to obtain the 60–80 mesh material used in our runs. On analysis, the catalyst was found to have 99.8% of the Na^+ exchanged. Bulk Si/Al ratio was determined by X-ray fluorescence, while framework Si/Al ratio was determined by ^{29}Si MAS-NMR. Crystallinity was checked by X-ray diffraction. The final catalyst was found to have bulk and framework Si/Al ratios of 2.5 and 4.49, respectively, and good crystallinity.

Runs were carried out in a fixed-bed gas-phase plug-flow reactor which has a 0.15-m catalyst bed containing the catalyst diluted with silica in order to minimize any thermal effects due to the heat of reaction. Details of the experimental apparatus and methodology have been presented previously (*26*). Thermal cracking experiments were carried out by pumping 2-methylpentane through a reactor packed with inert silica, which had been thoroughly cleaned with 36% HCl solution and rinsed with distilled water, in order to determine the extent and the contribution of noncatalytic cracking of 2-methylpentane. All reaction conditions and the amount of feed used were the same as used in the presence of the catalyst. Identification and analysis of products as well as the quantification of coke were carried out according to the procedures which have been presented previously (*26*).

TABLE 1

Initial Selectivities for Reaction of 2-Methylpentane on HY at 400°C

Product	Initial selectivity			
	Weight	Molar		
		Molecule	C	H
Hydrogen	.0004	.0172	—	.0344
Methane	.0030	.0161	.0161	.0644
Ethane	.0021	.0060	.0120	.0360
Ethylene	.0066	.0203	.0406	.0812
Propane	.0955	.1867	.5601	1.4936
Propylene	.0976	.1999	.5997	1.1994
Isobutane	.0595	.0882	.3528	.8820
n-Butane	.0229	.0340	.1388	.3470
C_4 olefins	.0117	.0180	.0720	.1440
Isopentane	.0814	.0973	.4865	1.1676
n-Pentane	.0069	.0082	.0410	.0984
C_5 olefins	.0065	.0080	.0400	.0800
2,3-DMButane	.0853	.0853	.5118	1.1942
3-Methylpentane	.4151	.4151	2.4906	5.8114
n-Hexane	.0472	.0472	.2832	.6608
C_6 olefins	.0487	.0498	.2991	.5982
Coke	.0086	.0101	.0528	.1031
Coke H/C ratio	—	1.96	—	—
Totals				
Experimental	.9990	1.3084	5.9971	13.9957
Theoretical	1.0000	N/A	6.00	14.00

RESULTS AND DISCUSSION

Chain Reaction Mechanism

Table 1 gives the initial weight and molar selectivities of all primary products in 2-methylpentane cracking on HY at 400°C. One can see that the initial products include paraffins in the range of C_1–C_5, olefins in the range of C_2–C_6, three C_6 isomers of the feed paraffin, hydrogen, and coke.

Table 2 was derived from Table 1 and shows molar selectivity ratios for pairs of product olefin (C_nH_{2n}) to the corresponding paraffin ($C_{6-n}H_{2(6-n)+2}$, $n = 2, 3, 4, 5, 6$).

Since the classical protolysis reaction splitting a molecule into two fragments must result in a value of one for all the product olefin-to-paraffin molar selectivity ratios, as shown by

$$C_6H_{14} \rightarrow C_nH_{2n+2} + C_{6-n}H_{2(6-n)}, \quad (1)$$

it is clear that protolysis alone does not account for the product distribution reported in Table 2.

There are other equally convincing reasons to conclude that the observed selectivity data proves that protolysis of 2-methylpentane is not the only initial process in the suite of reactions which take place during "catalytic cracking." For example, protolysis cannot explain the presence of initial C_5 paraffins. In order to explain this and the low olefin/paraffin ratios in the product distribution, the reaction mechanism has to include processes which are able to produce extra paraffins and/or remove olefins. To resolve these difficulties, we postulate the existence of a chain mechanism in catalytic cracking. A catalytic cracking chain mechanism, in keeping with the behaviour of the classical chain

TABLE 2

Molar Selectivity of Fragments for Reaction of 2-Methylpentane on HY at 400°C

Molar selectivity				Paraffin/olefin ratio
Paraffin		Olefin		
C_1	.0161	C_5	.0080	2.013
C_2	.0060	C_4	.0180	.333
C_3	.1867	C_3	.1999	.934
C_4	.1222	C_2	.0203	6.054
C_5	.1055			
Total	.4365		.2462	1.7729
H_2	.0172	C_6	0.498	.345
C_6	.5476			

mechanisms of gas-phase hydrocarbon pyrolysis, consists of the following essential steps.

1. Chain initiation. The conversion reaction is initiated on Brønsted acid sites by the direct protolysis of various C–C and C–H bonds, producing a smaller paraffin C_nH_{2n+2} in the gas phase and a complementary carbenium ion $C_{6-n}H_{13-2n}S^+$ on the catalyst surface

$$C_6H_{14} + SH \rightarrow C_nH_{2n+2} + C_{6-n}H_{13-2n}S, \quad n = 0, 1, 2, 3, 4, 5, \quad (2)$$

where C_6H_{14} is the feed molecule, SH is a Brønsted acid site, $C_{6-n}H_{13-2n}S^+$ is a carbenium ion associated with a Brønsted site, and C_nH_{2n+2} is a paraffin or hydrogen molecule (when $n = 0$) released into the gas phase.

We include $n = 5$ for completeness, without implying that methyl carbenium ions are important in the mechanism.

2. Chain propagation. The reaction is propagated by bimolecular processes between feed molecules and carbenium ions on the catalyst surface. One such bimolecular process is "hydrogen transfer" (reaction (3)), the other is "dimerization cracking" (reaction (4)):

$$C_nH_{2n+1}S^+ + C_6H_{14} \rightarrow C_nH_{2n+2} + C_6H_{13}S^+ \quad (3)$$

$$C_nH_{2n+1}S^+ + C_6H_{14} \rightarrow C_{n+x}H_{2(n+x)+2} + C_{6-x}H_{13+2x}S^+. \quad (4)$$

Obviously both of these bimolecular processes can produce an "extra" paraffin molecule, in the sense that a feed molecule is converted to a paraffin without producing an accompanying olefin. We call such events "chain propagation" process, implying that they may be repeated many times before a given site reverts to being a pristine Brønsted acid site.

When a carbenium ion is large enough, it can also undergo β-cracking to form an olefin and a smaller carbenium ion (*27*), for example,

$$C_6H_{13}S^+ \rightarrow C_nH_{2n} + C_{6-n}H_{13-2n}S^+, \quad n = 2, 3, 4, 5. \quad (5)$$

In 2-methylpentane cracking, the probability of this process occurring is very low, as we will see presently.

3. Chain termination. The reaction chain can be terminated by the desorption of any of the carbenium ions to yield an olefin. The reverse adsorption process will also take place as olefin products begin to appear in the gas phase:

$$C_nH_{2n+1}S^+ \rightarrow C_nH_{2n} + SH, \quad 2 < n < 6, \quad (6a)$$

$$C_nH_{2n} + SH \rightarrow C_nH_{2n+1}S^+. \quad (6b)$$

The net rate of reaction (6a) minus reaction (6b) must be equal to the rate of initiation by reaction (2) for the overall chain process to be at steady state. In the absence of β-cracking the selectivity for olefins will therefore provide a measure of the contribution of protolysis to overall conversion.

Carbenium ions will be involved in two other reactions. One is skeletal rearrangement or isomerization which is possible when an ion is large enough (reaction (7)), the other is coke formation, which also leads to catalyst decay (reaction (8)),

$$C_nH_{2n+1}S^+ \rightarrow i\text{-}C_nH_{2n+1}S^+, \quad n > 4, \quad (7)$$

$$C_nH_{2n+1}S^+ + C_mH_{2m+1}S^+ \rightarrow C_nH_{2n+2} + C_mH_{2m-1}S^+ + H^+S, \quad (8a)$$

where $i\text{-}C_nH_{2n+1}S^+$ is a skeletal isomer of the original carbenium ion $C_nH_{2n+1}S^+$, and $C_mH_{2m-1}S^+$ is a dehydrogenated precursor of coke.

The mechanism of catalyst decay and coke formation is an interesting and complicated subject in itself. It can be examined using (reaction (8a)), as we will show elsewhere. However, its inclusion here creates difficulties and complicates our pursuit of a quantitative description of product selectivity. Since the molar selectivity of coke is much smaller than those of product paraffins or olefins (Table 1), we will use a simplified coke forming reaction instead of reaction (8a),

$$C_6H_{14} \rightarrow m_kC_xH_y + m_HH_2, \quad (8b)$$

where C_xH_y represents the molecular formula of coke and will serve to balance our stoichiometry using the experimental values for x and y; m_k and m_H represent the number of moles of coke and hydrogen formed when 1 mole of feed is converted via reaction (8b). These will allow us to maintain mass and stoichiometric balances without examining the details of the coke forming processes.

We assume that the chain process reaches steady state in a very short time in comparison to the times accessible in our experiments. Therefore the chain reaction is assumed to be at steady state under our "initial" conditions. We note that such an assumption is in keeping with other such approximations, e.g., that an adsorption steady state exists between the gas phase and the catalyst surface at "initial" conditions for the cracking reaction.

Quantitative Treatment of Selectivity

The mathematical treatment of the mechanism consisting of reactions (2), (3), (4), (5), (6), and (8b) is described in detail in Appendix I (also see Table 3). To avoid distracting details, we will concentrate here on the conclusions which emerge from this procedure.

Reaction path probability (RPP). Scheme I shows the calculated probability of reaction (reaction path probability or RPP) as well as the product formation probability (PFP) for the various paths in the process of reactant conversion at 400°C. One can see that feed is consumed via three kinds of processes; path I is coke formation, path II is the initiation reaction, and path III is chain propagation. These overall reaction paths contribute to the total conversion in the ratio: I/II/III as 0.010/0.296/0.694. Each individual RPP in Scheme I represents the fraction of feed molecules which are converted to products via that specific reaction. It is obvious that feed is principally converted by chain propagation reactions, mainly leading to the isomerization of the feed molecule at 400°C. Using this kind of quantitative information we can examine the overall "cracking" reaction in great detail.

Probabilities of bond cleavage by protolysis (BCP). To compare the probabilities of protolysis of various C–C and C–H bonds, we can define the normalized bond cleavage probability (BCP) by initiation as

$$BCP_{0i}^{II} = \frac{RPP_{0i}}{\sum_{init} RPP_{0i}} \quad (9)$$

where i represents the ith mode of protolysis in the initiation process, RPP_{0i} is the probability of reactant conversion by the ith mode

TABLE 3

Reaction and Reaction Path Probabilities at 400°C

Reaction			RPP	
			Symbol	Value
C_6H_{14} + HS	→ H_2	+ $C_6H_{13}S$	X_{00}	0.006
C_6H_{14} + HS	→ CH_4	+ $C_5H_{11}S$	X_{01}	0.016
C_6H_{14} + HS	→ C_2H_6	+ C_4H_9S	X_{02}	0.006
C_6H_{14} + HS	→ C_3H_8	+ C_3H_7S	X_{03}	0.151
C_6H_{14} + HS	→ C_4H_{10}	+ C_2H_5S	X_{04}	0.117
C_6H_{14} + C_2H_5S	→ C_2H_6	+ $C_6H_{13}S$	X_{20}	0*
C_6H_{14} + C_2H_5S	→ C_3H_8	+ $C_5H_{11}S$	X_{21}	0*
C_6H_{14} + C_2H_5S	→ C_4H_{10}	+ C_4H_9S	X_{22}	0.005
C_6H_{14} + C_2H_5S	→ C_5H_{12}	+ C_3H_7S	X_{23}	0.091
C_6H_{14} + C_3H_7S	→ C_3H_8	+ $C_6H_{13}S$	X_{30}	0.036
C_6H_{14} + C_3H_7S	→ C_4H_{10}	+ $C_5H_{11}S$	X_{31}	0*
C_6H_{14} + C_3H_7S	→ C_5H_{12}	+ C_4H_9S	X_{32}	0.006
C_6H_{14} + C_4H_9S	→ C_4H_{10}	+ $C_6H_{13}S$	X_{40}	0*
C_6H_{14} + C_4H_9S	→ C_5H_{12}	+ $C_5H_{11}S$	X_{41}	0*
C_6H_{14} + $C_5H_{11}S$	→ C_5H_{12}	+ $C_6H_{13}S$	X_{50}	0.008
C_6H_{14} + $C_6H_{13}S$	→ C_6H_{14}	+ $C_6H_{13}S$	X_{60}	0.548
$C_6H_{13}S^+$	→ C_3H_6	+ $C_3H_7S^+$	X_{b63}	0*
C_6H_{14}	→ $m_kC_xH_y$	+ m_HH_2	X_{kc}	0.010
$C_jH_{2j+1}S^+$	→ C_jH_{2j}	+ HS	d_j	(see Table 1)

Sum of initiation probabilities:

$X_{00} + X_{01} + X_{02} + X_{03} + X_{04} = 0.296$

Note. Here initiation

- X_{0i} is the probability of feed consumption via the ith mode of protolysis.
- X_{jn} is the probability of feed consumption via the reaction of a feed molecule, with the surface ion $C_jH_{2j+1}S^+$ forming a paraffin molecule $C_{j-n}H_{2(j+n)+2}$ and a new surface ion $C_{6-(j+n)}H_{2(6-j-n)+1}S^+$.
- X_{60} is the probability of feed consumption via the production of isomers of the feed molecule.
- X_{kc} is the probability of feed consumption by the formation of coke.
- X_{b63} is the probability of propylene production from the β-scission of $C_6H_{13}S^+$ ion.
- d_j is the molar selectivity for olefin C_jH_{2j} production from the desorption of $C_jH_{2j+1}S^+$ in a termination reaction.
- * a zero value indicates values less than 0.0005.

of initiation, $\Sigma_{init} RPP_{0i}$ is the total of all probabilities of reactant conversion by initiation, and BCP_{0i}^{II} is the probability of cleaving bond i by protolysis.

Scheme II shows the calculated BCP values for various bonds (see Appendix II for details of the calculation procedures). One can see that the protolysis of bonds in the feed molecule on Brønsted acid site at 400°C follows the order

$$C_t\text{–}C_s > C_s\text{–}C_s > (C_t\text{–}C_p \text{ or } C_s\text{–}C_p) > C_t\text{–}H \quad (10)$$

in the ratio 0.510/0.416/0.054/0.020. As expected, the tertiary–secondary C–C bond is

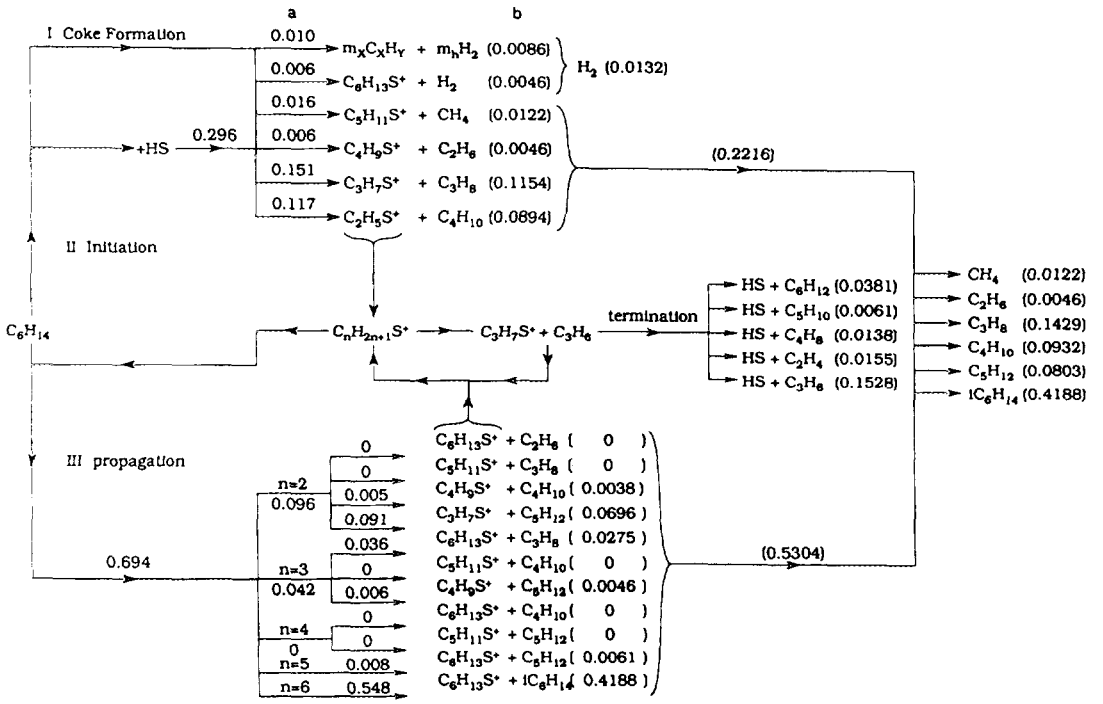

SCHEME I. (a) Reaction path probability (RPP) at 400°C. (b) Product formation probability (PFP) at 400°C.

easiest to break, while the C–H bond is the most difficult to crack.

Isomerization mechanism and isomerization probability (IC_6). The events involved in i-$C_6H_{13}S^+$ ion formation throw a new light on the mechanism of paraffin isomerization. Although there is evidence that isomerization of paraffins can occur on Lewis acid sites in the superacid systems P_2O_5/Al_2O_3 and $AlCl_3/Al_2O_3$ (*7*, *28*), in our case it seems more reasonable to think that the $C_6H_{13}S^+$ ion is associated with a Brønsted site which is also responsible for the appearance of C_6H_{12} products. These can only be formed by the desorption of a $C_6H_{13}S^+$ ion residing on a Brønsted base. Part of the total $C_6H_{13}S^+$ ion population is obviously produced by initiation involving the protolysis

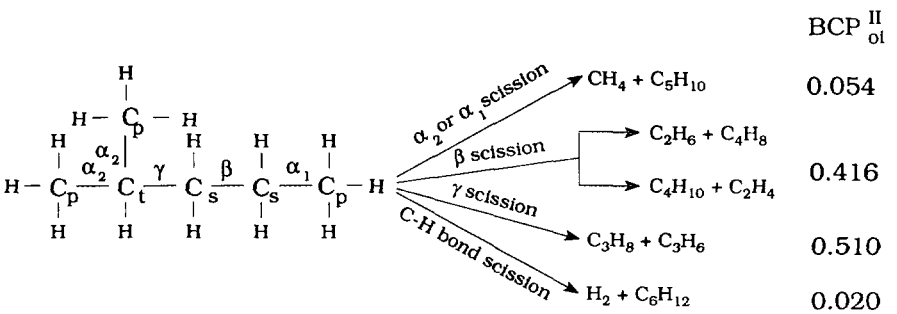

SCHEME II. Bond cleavage probability (BCP) by protolysis at 400°C.

of a tertiary hydride and the formation of initial molecular hydrogen, but most is formed by hydrogen transfer from a feed molecule during chain propagation. Once formed, the parent ion undergoes skeletal rearrangement and then abstracts an H^- from a subsequent feed molecule to produce an i-C_6H_{14} paraffin and a new $C_6H_{13}S^+$ ion. This mechanism readily accounts for all the i-C_6 paraffins in the products. As to how long the isomerization chain can propagate, this depends on the various competitive reactions involving the $C_6H_{13}S^+$ ion, such as reactions (5) and (6a). We define the isomerization probability for C_6 ions as

$$IC_6 = \frac{C_6H_{13}S^+ \text{ isomerization probability}}{\Sigma C_6H_{13}S^+ \text{ ion reaction probabilities}} \quad (11)$$

From the data in Table 1 and further to the discussion in Appendix I, we can calculate that IC_6 has a value of 0.916 (see Appendix III for details). It seems that the $C_6H_{13}^+$ carbenium ion is quite stable to both β-cracking and desorption at 400°C. It prefers to rearrange and wait until it abstracts an H^- from a feed molecule in order to desorb as an isomerized paraffin.

Overall kinetic chain length (KCL). The overall kinetic chain length (KCL) is defined as

$$KCL = \frac{\text{overall rate}}{\text{rate of initiation}}. \quad (12)$$

KCL represents the average number of chain events which follows an initiation event. We calculate in Appendix IV the value of KCL to be 3.34 at 400°C. This indicates that for each feed molecule protolyzed by a pristine Brønsted site a further 2.34 molecules react by chain processes. This in turn means that chain processes, not protolysis by the pristine sites, are responsible for ~70% of the total conversion.

The stoichiometry of paraffin cracking. Generally a paraffin undergoing cracking will produce paraffins, olefins, coke, and aromatics. Most of the time coke, aromatics and products larger than the feed constitute minor products and we will ignore their formation for the moment. In that case the mechanism described in Appendix I can be simplified to

$$m_fP_f \rightarrow m_iP_i + m_cP_c + m_tO_t + m_bO_b, \quad (13)$$

where P_f is the feed paraffin; P_i is a product paraffin formed by initiation; P_c is a product paraffin formed by chain propagation; O_t is a product olefin formed by chain termination; O_b is a product olefin formed by β-cracking; and m_f, m_i, m_c, m_t, and m_b are the corresponding stoichiometric coefficients.

In the absence of chain propagation, Eq. (13) reduces to

$$m_fP_f \rightarrow m_iP_i + m_tO_t \quad (14a)$$

where

$$m_f = m_i = m_t. \quad (14b)$$

Thus for a process consisting solely of protolysis reactions one expects that the total number of paraffins formed will correspond to the total number of feed molecules converted. Moreover, paraffins and corresponding olefins must be formed in a one-to-one ratio.

If the process consists of both protolysis and chain reactions, inspection of the mechanism in Appendix I shows that for every paraffin molecule reacted a paraffin is formed. That is,

$$m_f = m_i + m_c. \quad (15)$$

The consequence is that the sum of initial molar paraffin selectivities (including initial hydrogen production) must be equal to one. An elaboration of this requirement is that in cases where coke is present in significant amounts but is not dehydrogenated significantly, the sum of all initial molar paraffin selectivities plus the molar coke selectivity must equal one. In cases where total paraffin selectivity is greater than one, the extra paraffins come from the saturation of olefins by coke, causing the coke to be dehydroge-

nated. Such a situation arises in *n*-nonane cracking (*31*).

Formation of initial coke and hydrogen. Initial molecular hydrogen can be formed in the following ways: (a) thermal cracking of gas phase species, (b) protolysis of a C–H bond in the feed paraffin, and (c) thermal elimination from surface species in association with the formation of coke (*13*). In the case of 2-methylpentane cracking (a) is negligible, since we have not detected any hydrogen in blank runs. Assuming that the initial coke is produced via reaction (8b) instead of (8a), it is possible to separate the hydrogen produced by (b) and (c). From the total mass balance and from analysis, we find the H/C molar ratio in the initial coke to be 1.96 and separate the total initial molar selectivity of hydrogen produced by (b) and (c) to obtain the RPP values of .0060 and 0.0112 for (b) and (c), respectively. The assumption that the stoichiometric coefficients in (8b) are equal, i.e., $m_k = m_H$, gives the average molecular weight of initial coke as 74.8 with the formula $C_{5.4}H_{10.5}$. This represents the loss of about 0.5 atoms of hydrogen per molecule of feed deposited as coke. The details of this calculation appear in Appendix V. The rate of coke formation will be sensitive to the rate of the reaction shown in Eq. (8a) and hence to surface concentrations of the various ions and their surface residence times.

Influence of Temperature on Selectivity and Mechanism

Thermal cracking. The thermal cracking at 400, 450, and 500°C resulted in conversions of 2-methylpentane of 0.332, 0.964, and 1.5%, respectively, for a run duration of 20 min, and the product distribution was different from that due to catalytic cracking. Thermal products consisted mainly of paraffins and olefins in the range C_1–C_5. Their amounts varied almost linearly with time on stream, as shown in Fig. 1. Molecular hydrogen was not detected as a thermal product. The difference in product distribution between thermal and catalytic cracking at these three temperatures suggests that thermal cracking proceeds via a different mechanism, presumably via a free-radical chain mechanism. The presence of thermal cracking products shows, however, that thermal products can influence the interpretation of initial selectivity data. For this reason initial selectivities of catalytic products were determined by subtracting the thermal product yields from the total yields observed experimentally.

Catalytic cracking. Product types and initial selectivity data for primary products at 400, 450, and 500°C were obtained by interpolating OPEs (*24*) and are listed in Tables 4–6. The initial products include C_1–C_6 compounds (paraffins or olefins), hydrogen, and coke at all three temperatures. Figures 2 and 3 show some examples of the OPE curves of primary products.

At 400°C, only small amounts of molecular hydrogen were observed, and the initial products consisted mainly of C_6 isomers. The C_6 olefins, at all temperatures, consisted largely of 2-methyl-2-pentene, *cis*- and *trans*-3-methyl-2-pentene, 2-methyl-1-pentene, and 2,3-dimethyl-2-butene as shown in Table 7. The proportion of these C_6 olefin isomers in the product did not change significantly with reaction temperature, in agreement with results reported elsewhere (*25*). It is interesting to note that the major C_6 olefinic products have skeletal structures similar to the C_6 paraffinic products shown in Table 6. This supports the postulate that the two types of products arise from the same ions present on the surface undergoing alternative types of desorption.

At 450°C, an appreciable amount of hydrogen and an increase in C_3–C_5 species was noted. This was accompanied by a decline in C_6 paraffin isomers. At 500°C, the product distribution continued this trend; propylene and propane now represent ~50 wt% of the primary products compared to 20 wt% at 400°C (Table 5).

In addition to primary products, the cracked material contained secondary

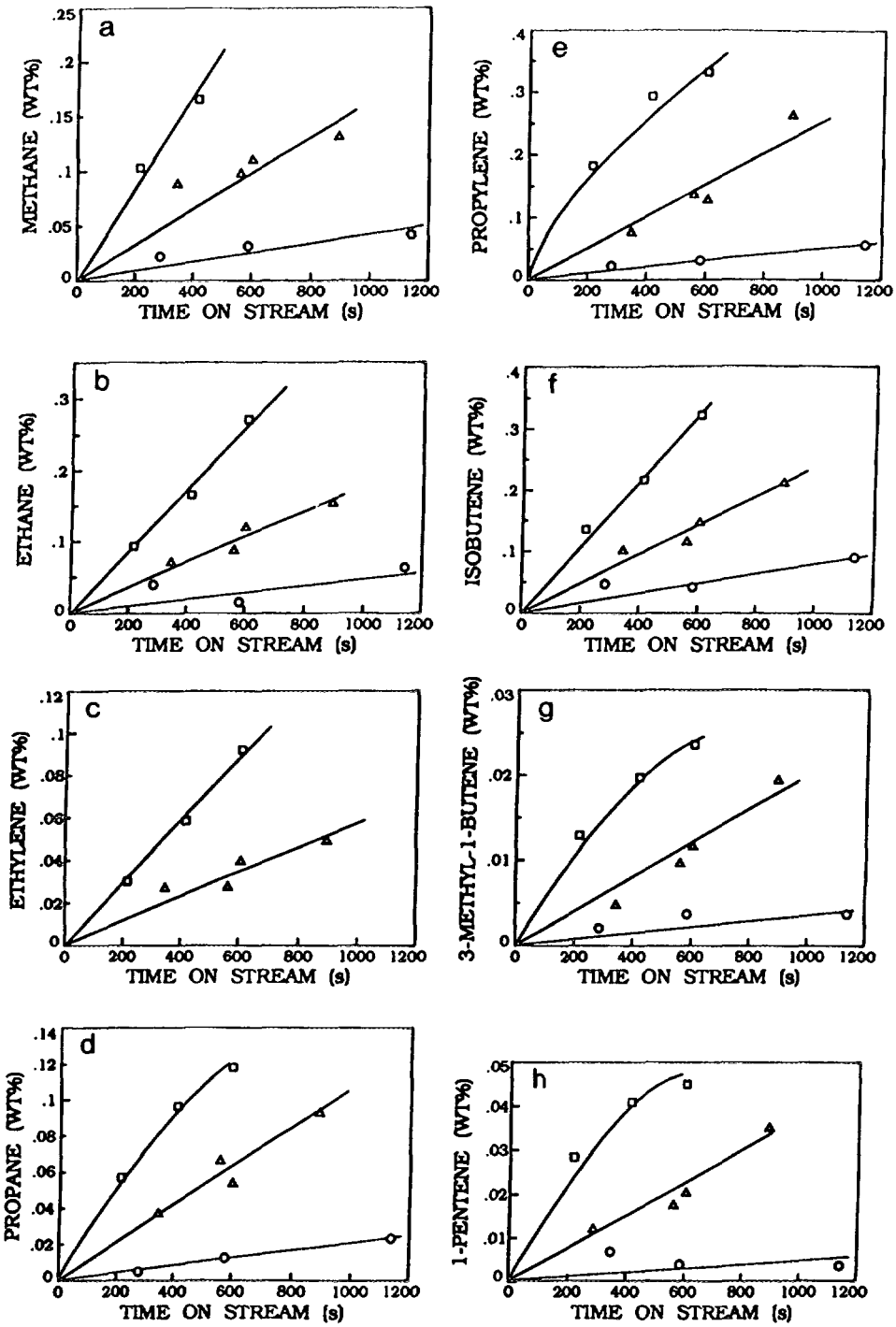

FIG. 1. Yield of thermal products from 2-methylpentane at various temperatures vs time on stream: (a) methane, (b) ethane, (c) ethylene, (d) propane, (e) propylene, (f) isobutene, (g) 3-methyl-1-butene, and (h) 1-pentene. Temperature: (○) 400°C; (△) 450°C, and (□) 500°C.

TABLE 4

Products[a] from Cracking Reactions of 2-Methylpentane over USHY in the Temperature Range 400 to 500°C

Product	Temperature (°C)		
	400	450	500
Hydrogen	1S	1S	1S
Methane	1S	(1 + 2)S	(1 + 2)S
Ethane	1S	(1 + 2)S	(1 + 2)S
Ethylene	1S	1S	(1 + 2)S
Propane	(1 + 2)S	(1 + 2)S	(1 + 2)S
Propene	1U	1U	1U
Isobutane	(1 + 2)S	(1 + 2)S	(1 + 2)S
n-Butane	(1 + 2)S	(1 + 2)S	(1 + 2)S
Isobutene	1S	1S	1S
trans-2-butane	1S	1S	1S
cis-2-butane	1S	1S	1S
Isopentane	(1 + 2)S	(1 + 2)S	(1 + 2)S
n-Pentane	(1 + 2)S	(1 + 2)S	(1 + 2)S
C_5-Olefins	1S	1S	1S
2,3-Dimethylbutane	1S	1U	1U
3-Methylpentane	1U	1U	1U
n-Hexane	1S	1U	1U
C_6-Olefins	1U	1U	1U
Coke	(1 + 2)S	(1 + 2)S	(1 + 2)S

[a] 1, primary; 2, secondary; S, stable; U, unstable.

products (Table 8). The secondary products were found to decrease with increasing reaction temperature and consisted largely of 2,2-dimethylbutane, methylcyclopentane, C_7 paraffins and olefins, C_8 olefins, and C_7–C_9 aromatics. Aromatics with carbon numbers >9, mainly alkylated naphthalenes, were relatively minor products. The C_7 paraffins consisted essentially of 2-methylhexane, 3-methylhexane, and heptane. Aromatization led mainly to the formation of toluene, dimethylbenzenes and trimethylbenzenes. The aromatics were detected in the liquid products at conversions higher than 4% and their yield increased sharply with increasing conversion. On the other hand, the yield of 2,2-dimethylbutane, methyl-cyclopentane, and C_7 paraffins and olefins at first increased with increasing conversion, but levelled off at conversions greater than 25%. This indicates that these products are unstable under the reaction conditions and react to form subsequent products, perhaps coke and aromatics. Figure 4 shows examples of secondary product OPEs.

Effect of temperature on RPPs and BCPs. The reaction pathway probabilities (RPPs) at three temperatures have been calculated according to the proposed procedure (Appendix I) and are presented in Table 9. Examination of the RPPs shows that the contribution to conversion by pure protolytic processes (entries 1–5) is small at 400°C, but grows in importance with increasing temperature. Protolysis on pristine sites accounts for about 28% of the total conversion at 400°C and about 67% at 500°C.

Table 10 presents the probabilities of protolysis for each mode of reaction relative to the total rate of protolysis. These are the bond cracking probabilities (BCPs) described in Eq. (9). We see that the C–C bond next to the tertiary carbon is most readily broken, contributing >50% of all protolysis products at all temperatures. In-

TABLE 5

Initial Weight Selectivities for Cracking Products of 2-Methylpentane over USHY in the Temperature Range 400 to 500°C

Product	Temperature (°C)		
	400	450	500
Hydrogen	0.0003	0.0008	0.0023
Methane	0.0027	0.0028	0.0031
Ethane	0.0017	0.0016	0.0030
Ethylene	0.0059	0.0068	0.0124
Propane	0.0920	0.1510	0.2170
Propene	0.0972	0.1695	0.2900
Isobutane	0.0560	0.0609	0.0820
n-Butane	0.0198	0.0214	0.0217
Isobutene	0.0040	0.0090	0.0220
trans-2-butane	0.0038	0.0041	0.0094
cis-2-butane	0.0020	0.0030	0.0080
Isopentane	0.0798	0.0870	0.0950
n-Pentane	0.0063	0.0055	0.0033
C_5-Olefins	0.0065	0.0080	0.0032
2,3-Dimethylbutane	0.0896	0.0690	0.0382
3-Methylpentane	0.4326	0.3045	0.1210
n-Hexane	0.0490	0.0460	0.0210
C_6-Olefins	0.0400	0.4200	0.4100
Coke	0.0080	0.0074	0.0065
Total	0.9972	1.003	1.005

TABLE 6

Initial Molar Selectivities[a] for Products from Reaction of 2-Methylpentane on USHY at Various Temperatures

Product	Temperature (°C)		
	400	450	500
Hydrogen	0.0129	0.0344	0.0989
Methane	0.0145	0.015	0.0167
Ethane	0.0049	0.0046	0.0086
Ethylene	0.0181	0.0209	0.0381
Propane	0.1801	0.2956	0.4248
Propene	0.1990	0.3471	0.5939
Isobutane	0.0830	0.0903	0.1216
n-Butane	0.0294	0.0317	0.0322
Isobutene	0.0061	0.0138	0.0038
trans-2-butene	0.0058	0.0063	0.0144
cis-2-butene	0.0031	0.0046	0.0123
Isopentane	0.0953	0.1039	0.1135
n-Pentane	0.0075	0.0066	0.0039
C_5-Olefins	0.0080	0.0098	0.0039
2,3-Dimethylbutane	0.0896	0.0690	0.0387
3-Methylpentane	0.4326	0.3045	0.1210
n-Hexane	0.0490	0.0460	0.0210
C_6-Olefins	0.0410	0.0430	0.0420
Coke	0.0080	0.0074	0.0065
Totals	1.2879	1.4545	1.7458
Sum of paraffins	0.9859	0.9672	0.9020

[a] Initial molar selectivities were calculated from initial weight selectivities in Table 5 using the relationship:

$$\text{Molar selectivity} = \text{weight selectivity} \cdot \frac{\text{molecular wt. of feed}}{\text{molecular wt. of product}}$$

creasing temperature from 400 to 500°C enhances the probability of C–H bond protolysis from 1.8 to 13.8%; the protolysis of both α and β C–C bonds decreases by a factor of 2. These trends reflect differences in activation energy for the various reactions and indicate that the hydrogen bond requires the highest activation energy for protolysis.

We note that the RPPs of bimolecular disproportionation (Entries 6–11 in Table 9) generally decrease with increasing temperature. This can be attributed to the rapid desorption 2-methylpentyl ions and to β-cracking at higher temperatures. We see that the value of X_{b63} increases from 0 to 7% with increasing temperature from 400 to 500°C.

We clearly see a shift in reaction mechanism from hydride transfer and chain cracking at low reaction temperatures to protolysis at higher temperatures. In examining the details of this overall shift, we should note that some processes, such as reactions 6 and 9 in Table 9, seem to buck the trend.

Effect of temperature on paraffin/olefin ratio. From Table 6 we see that the total molar selectivity of the products increases from 1.29 to 1.75 with increasing temperature from 400 to 500°C, but the sum of paraffin plus hydrogen selectivities stays almost constant at a value of 1. This means that raising the temperature results in an increase of the proportion of olefins in the products. Figure 5a shows the increase of olefin/paraffin ratio in products with rising temperature. In terms of the chain mechanism, olefins are mainly produced from the desorption of carbenium ions, i.e., the termination of reaction chains. An increase in the rate of the termination reaction must lead to a shortening of reaction chain length, as presented in Fig. 5b.

Effect of temperature on isomerization. We find from Table 6 that except for C_6 isomeric paraffins and C_6 olefins, the molar selectivity of all other initial products increases with rising temperature. For C_6 isomeric paraffins, both molar selectivity and product formation probability (PFP) decrease with rising temperature. For C_6 olefins, the molar selectivity stays constant but the PFP decreases with rising temperature, as presented in Fig. 6a. Since we have postulated that the production of C_6 isomeric paraffins and olefins involves the same carbenium ions ($C_6H_{13}S^+$), the best way to understand the effect of temperature on isomerization is to investigate the competition of those processes for the surface species. Figure 6b shows the variation of IC_6 (Eq. (15)) with temperature. We conclude that the abrupt drop of isomerization selectivity with rising temperature re-

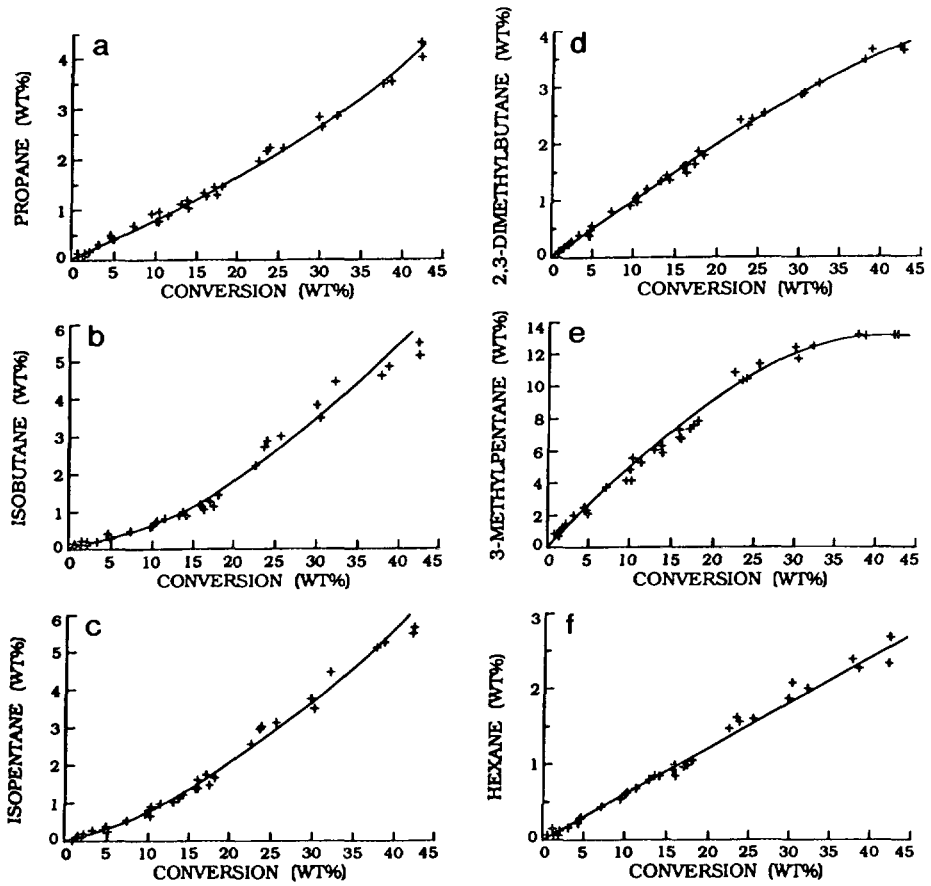

FIG. 2. Optimum performance envelopes for products of reaction of 2-methylpentane on USHY at 400°C: (a) propane, (b) isobutane, (c) isopentane, (d) 2,3-dimethylbutane, (e) 3-methylpentane, and (f) hexane. Catalyst-to-reactant ratio: 0.0002–0.104.

sults from a decrease of the lifetime of $C_6H_{13}S^+$ ions and the emergence of β-cracking of these ions at higher temperature.

Effect of temperature on the formation of coke and hydrogen. The probability of coke formation (Table 9) was found to decrease with rising temperature. Since coke is the product of bimolecular reactions between surface species (Eq. (8a)), its decreased rate of formation agrees with the postulate that there are fewer such species at high temperature. We also see an increase in the probability for hydrogen production with temperature (Table 9). However, since the value of $X_{(0)}$ at 500°C is still less than the molar selectivity of hydrogen at this temperature (Table 6), we conclude that there is still a small part of hydrogen produced in association with coke formation (Appendix V). This contribution, however, is much smaller at the higher temperatures, indicating that coke dehydrogenation is more prevalent at low temperatures.

Apparent Activation Energies

To compare the apparent activation energies of individual reactions taking place during 2-methylpentane cracking, we first calculated the individual reaction rates (IRR). This is done by multiplying the appropriate

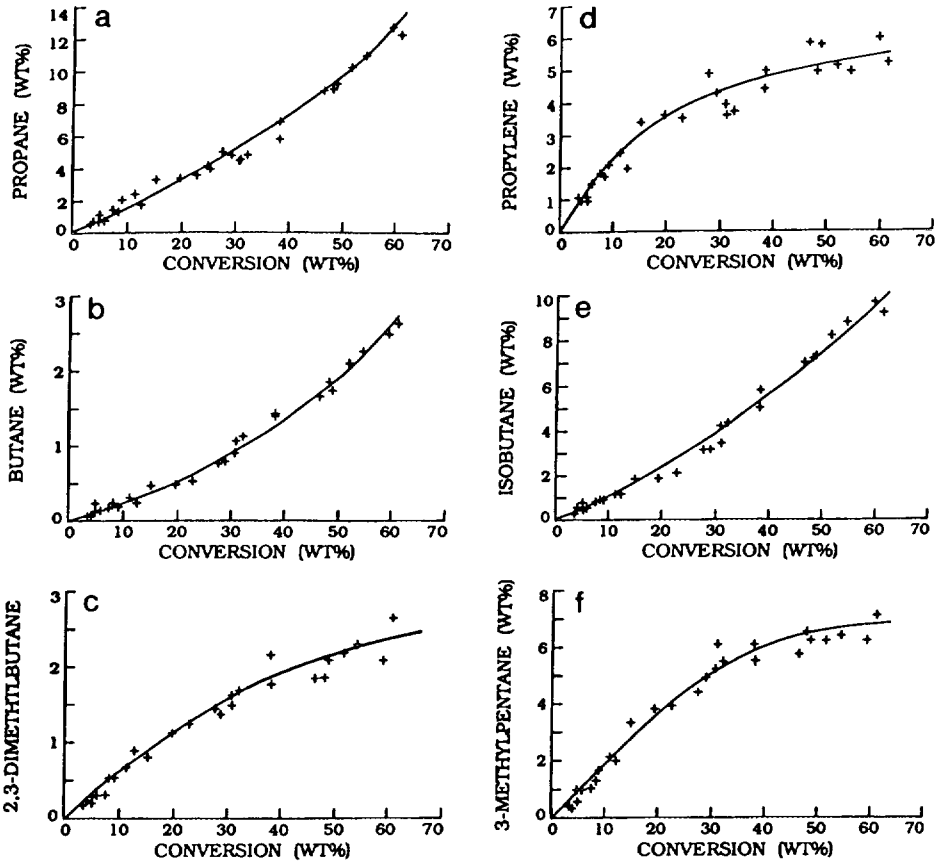

FIG. 3. Optimum performance envelopes for products of reaction of 2-methylpentane on USHY at 500°C: (a) propane, (b) butane, (c) 2,3-dimethylbutane, (d) propylene, (e) isobutane, and (f) 3-methylpentane. Catalyst-to-reactant ratio: 0.001–0.108.

RPPs listed in Table 9 by the total initial rate of reaction, obtained from the fitting of the overall rate of conversion by a suitable kinetic rate expression (see Ref. (*22*) for the rate expression used):

$$r_j = \mathrm{RPP}_j * \sum_i r_i. \qquad (11)$$

From the values of r_j listed in Table 11, plots of ln r_j vs $1/T$ have been generated, as shown in Fig. 7. From the slopes of the plots the activation energies for individual reactions have been calculated and are tabulated in Table 11. We note that the protolysis reaction leading to H_2 formation shows a higher activation energy than that of the other protolysis processes. In general, the activation energies for monomolecular processes are higher than those of disproportionation reactions. Among bimolecular processes lower activation energies are observed for the reactions in which $C_3H_7S^+$ or $C_6H_{13}S^+$ abstracts a hydride (H^-) from a feed molecule. Note, however, that reactions 6 and 9 show very high activation energies, explaining why these two processes buck the trend of decreasing importance of bimolecular processes at high temperatures.

CONCLUSIONS

In this paper and the preceding paper on the kinetics of chain cracking (*22*), we

TABLE 7

Initial Molar Selectivities for C_6-Olefins from Reaction of 2-Methylpentane over USHY at Various Temperatures

Product	Temperature (°C)		
	400	450	500
1-Hexene	—	—	0.0011
cis-2-Hexene	0.0012	0.0018	0.0020
trans-2-Hexene	0.0031	0.0038	0.0038
cis-3-Hexene	0.0017	0.0023	0.0024
trans-3-Hexene	0.0011	0.0016	0.0016
2-methyl-1-pentene	0.0041	0.0060	0.0048
2-methyl-2-pentene	0.0094	0.0083	0.0080
cis-3-methyl-2-pentene	0.0057	0.0053	0.0051
trans-3-methyl-2-pentene	0.0057	0.0053	0.0051
2,3-Dimethyl-1-butene	0.0014	0.0018	0.0019
2,3-Dimethyl-2-butene	0.0034	0.0032	0.0027
Total	0.0410	0.0428	0.0419

have established a quantitative methodology for the detailed analysis of hydrocarbon cracking. The methods are general, founded on well documented mathematical and experimental methods, and are capable of yielding detailed information on the mechanism of any catalytic cracking reaction.

In the cracking of 2-methylpentane, we have been able to determine the reaction probability of each individual pathway and the relative probabilities of protolysis of the various bonds. At 400°C, for example, the probability of cracking the tertiary–secondary carbon–carbon bond is higher than that of cracking a secondary–secondary bond. It may, however, come as a surprise that cracking of an α bond is some 10 times less likely, though not zero, as shown by our calculation of its BCP as listed in Table 10. The lowest probability of protolysis is that of a C–H bond which is much less than that of cracking of an α C–C bond. Even at that, we expect that only the tertiary C–H bond is protolyzed and the other C–H bonds have an even lower probability of cracking.

Overall the conversion of a 2-methylpentane at 400°C proceeds by protolysis only to the extent of some 30%. The rest of the conversion is due to bimolecular reactions between surface carbenium ions and gas-phase feed molecules. Such chain reactions are responsible for the production of excess paraffins and other "anomalies" in the product distribution. They explain the production of C_5H_{12} without a corresponding olefin, the production of i-C_6, and the olefin to paraffin ratios for various product pairs such as $C_2:C_4$ and $C_3:C_3$. Moreover, the chain mechanism explains all these phenomena in a simple, logical, consistent, and quantitative way.

From the details of the chain reaction probabilities, we see that CH_3^- transfer does not take place at all in this system. Other fragments such as $C_2H_5S^-$ or H^- are abstracted by the various carbenium ions in varying degrees. The probability for the abstraction of a given moiety differs significantly depending on the ion present on the surface. This is to be expected, as the reaction probability is related to the rate of reaction and is therefore composed of terms accounting for both the rate constant of the reaction and the concentration

TABLE 8

Yield (wt%) of Secondary Products from Reaction of 2-Methylpentane at 25% Conversion

Product	Temperature (°C)		
	400	450	500
2,2-Dimethylbutane	.1140	.1050	.0414
Methylcyclopentane	.0430	.0240	.0060
C_7-Paraffins	.3930	.2050	.1580
C_7-Olefins	.1580	.1070	.0820
Toluene	.0450	.0420	.0370
C_8-Olefins	.0880	.0400	.0123
Dimethylbenzenes	.2180	.1880	.1080
Trimethylbenzenes	.0933	.0750	.0450
Ethyldimethylbenzene	.0230	.0170	.0080
Methylnaphthalenes	.0020	.0030	.0030
Dimethylnaphthalenes	.0030	.0040	.0040
Trimethylnaphthalenes	.0030	.0040	.0020
Total	1.1833	.8140	.5067

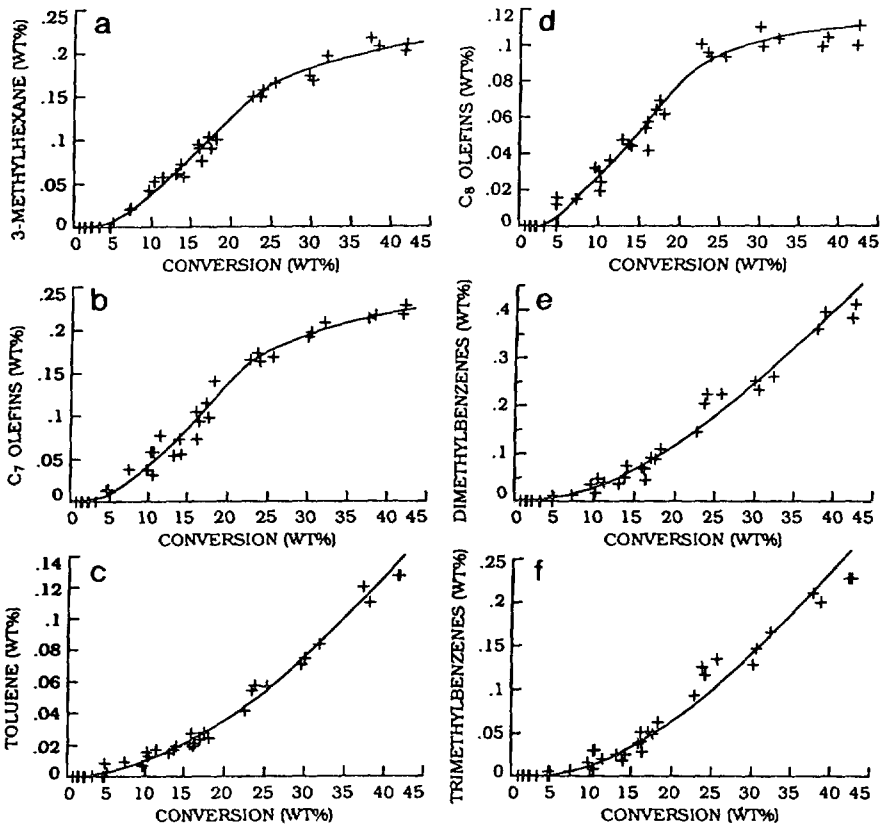

FIG. 4. Yield of secondary products vs conversion of 2-methylpentane on USHY at 400°C: (a) 3-methylhexane, (b) C_7 olefins, (c) toluene, (d) C_8 olefins, (e) dimethylbenzenes, and (f) trimethylbenzenes. Catalyst-to-reactant ratio: 0.001–0.104.

of the given carbenium ion on the surface. On top of these classical considerations, stearic effects are likely to play a major role in disproportionations involving the stearically constrained, surface-resident carbenium ions. We find, for example, that ethyl ions and propyl ions are active in various abstractions, while butyl ions seem to take no part in such processes. $C_5H_{11}S^+$ and $C_6H_{13}S^+$ abstract only H^- and nothing else. We will reserve further discussion of the meaning of the various probabilities of disproportionation until we have had a chance to examine such probabilities in a variety of molecules.

It seems that in general the preferred product of disproportionation lies in the C_4–C_5 range. In some reactions, however, such as the cracking of *n*-hexane, products larger than the feed appear in the gas phase (*29*). This may be due to the transfer of CH_3^- or $C_2H_5^-$ to parent carbenium ions in cases where there is no weakly bonded hydrogen in the feed molecule.

We note that without the insights offered by the concept of chain reactions, even detailed studies of catalyst selectivity can only produce a confused picture of the mechanism involved or of the effects of such variables as temperature. It is clear from Appendix I that a given initial product can be formed by both protolysis and by various chain processes. For example, at 400°C by using the results shown in Table 3 we obtain

TABLE 9[a]

Reaction Pathway Probabilities[b] for the Reactions of 2-Methylpentane over USHY at Various Temperatures

Entry no.	RPP	Temperature (°C)		
		400	450	500
1	X_{00}	0.005	0.026	0.092
2	X_{01}	0.014	0.015	0.017
3	X_{02}	0.005	0.005	0.009
4	X_{03}	0.148	0.266	0.418
5	X_{04}	0.109	0.117	0.133
Total initiation		0.281	0.429	0.669
6	X_{22}	0.003	0.005	0.021
7	X_{23}	0.089	0.090	0.074
8	X_{30}	0.031	0.029	0.007
9	X_{32}	0.007	0.015	0.031
10	X_{50}	0.006	0.005	0.013
11	X_{60}	0.571	0.419	0.181
12	X_{kc}	0.012	0.008	0.004
13	X_{b63}	0.000	0.017	0.070
Kinetic chain length		3.56	2.33	1.49
	Total	0.9998	0.9994	0.9998

[a] Results at 400°C may be compared to those reported in Table 3 for the same feedstock and catalyst but done in a different apparatus by a different operator.

[b] All RPPs not listed here were found to be equal to zero using the constrained linear solution of equations shown in Table 6.

the proportion of the total propane which is formed by protolysis from $X_{03}/(X_{03} + X_{21} + X_{30})$. Overall propane therefore comes from

$$C_6H_{14} + HS \rightarrow C_3H_7^+S + C_3H_8$$

81% by protolysis

$$C_6H_{14} + C_3H_7^+S \rightarrow C_6H_{13}^+S + C_3H_8$$

19% by propagation,

while butanes come from

$$C_6H_{14} + HS \rightarrow C_2H_5^+S + C_4H_{10}$$

96% protolysis

TABLE 10

Bond Cracking Probabilities at Various Temperatures

Bond		Temperature (°C)		
		400	450	500
C–H	$H–C_t + (H–C_s) + (H–C_p)$	0.018	0.061	0.138
γ	$C_t–C_s$	0.527	0.620	0.625
β	$C_s–C_s$	0.406	0.284	0.212
α	$C_s–C_p + (C_t–C_p)$	0.050	0.035	0.025

Note. C_p is a primary carbon, C_s is a secondary carbon, and C_t is a tertiary carbon.

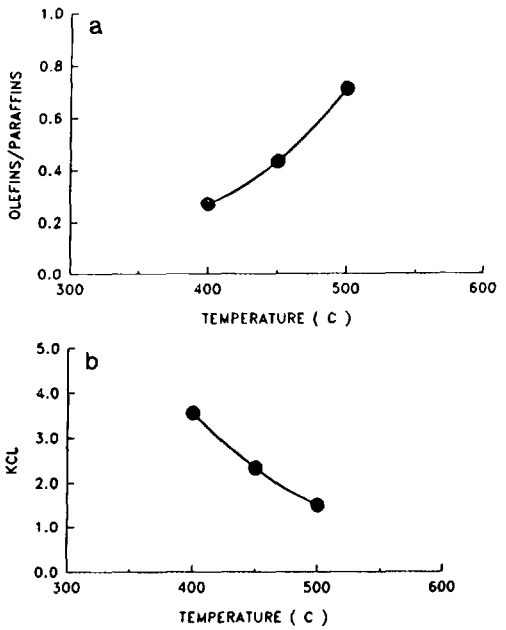

FIG. 5. (a) Olefins/paraffins ratio for 2-methylpentane cracking on HY vs temperature. (b) Kinetic chain length for 2-methylpentane cracking on HY vs temperature.

$$C_6H_{14} + C_2H_5^+S \rightarrow C_4H_9^+S + C_4H_{10}$$
4% chain propagation,

and pentanes come from three separate chain propagation reactions:

$$C_6H_{14} + C_2H_5^+S \rightarrow C_3H_7^+S + C_5H_{12}$$
86% chain propagation

$$C_6H_{14} + C_3H_7^+S \rightarrow C_4H_9^+S + C_5H_{12}$$
6% chain propagation

$$C_6H_{14} + C_5H_{11}^+S \rightarrow C_6H_{13}^+S + C_5H_{12}$$
8% chain propagation.

Interpreting the effects of any reaction variable such temperature in terms of the overall product selectivities, even initial product selectivities, can only lead to confusion.

The big surprise is that β-cracking seems to play no role in the conversion of 2-methylpentane at 400°C. We are used to interpreting catalytic cracking as a process mostly proceeding by β-cracking, yet in this reaction, nearly all the other products come from protolysis or from chain reactions. The participation of β-cracking increases with temperature, as shown in Table 9.

Temperature has a profound effect on the selectivity and the mechanism in 2-methylpentane cracking on HY zeolite. As a result, increasing reaction temperature from 400 to 500°C leads to:

(1) A large increase of the RPPs of protolysis (from 28 to 67%) with a large decrease of the RPPs of chain processes (from 71 to 33%) because the agents of chain propagation, carbenium ions, tend to desorb as olefins at higher temperatures. This change in reaction mechanism results in the shortening of overall kinetic chain length from 3.4 to 1.5 and the increase of product olefin/paraffin molar ratio from 0.28 to 0.74.

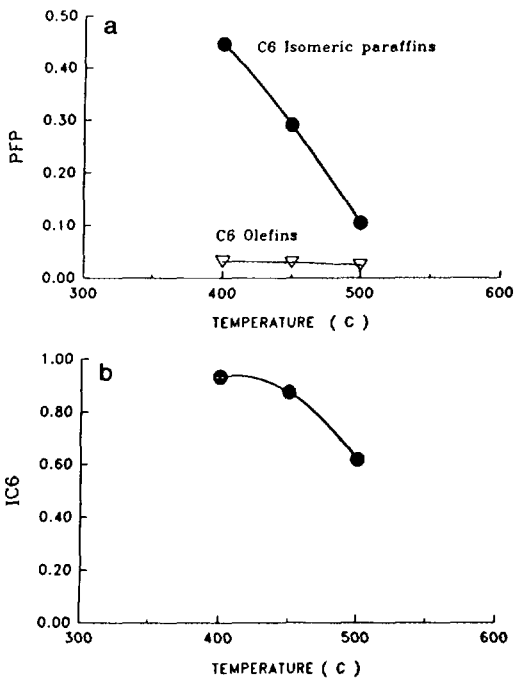

FIG. 6. (a) Formation probability of C_6 isomeric paraffins and olefins in 2-methylpentane cracking on HY vs temperature. (b) Probability of $C_6H_{13}S^+$ ions forming i-C_6H_{14} vs temperature.

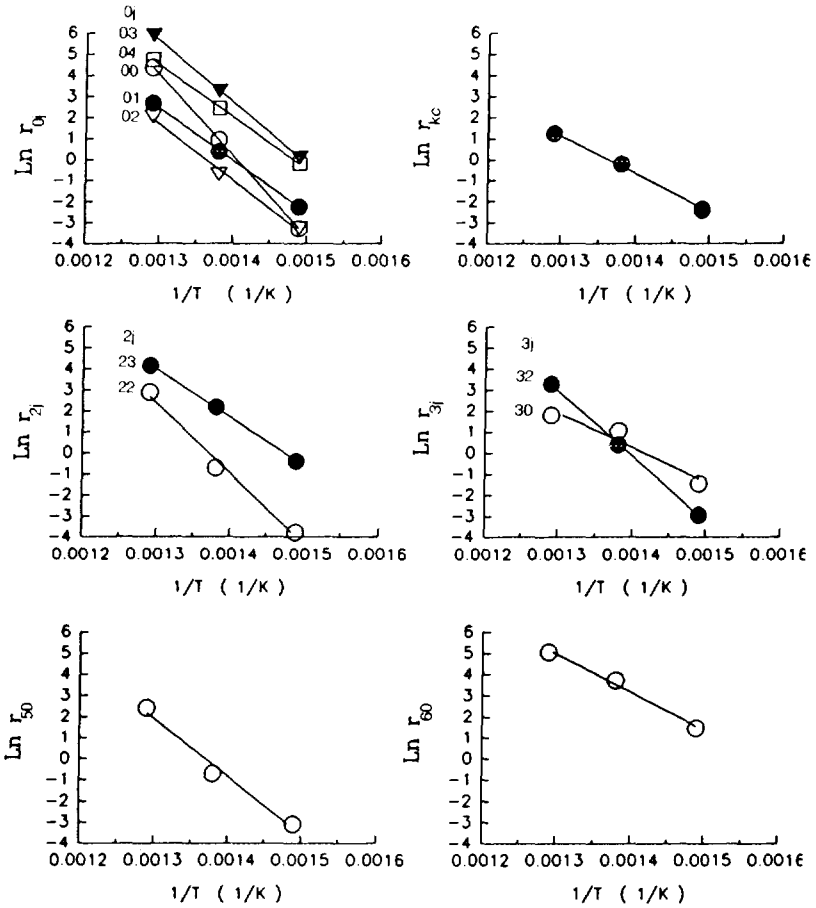

FIG. 7. Arrhenius plots for various elementary processes in 2-methylpentane cracking on HY.

(2) An obvious change of the distribution of bond cracking probability (BCP), especially the probability of C–H bond protolysis.

(3) A decrease of the IC_6 from 93 to 62%.

(4) A decrease of the RPP of coke formation from 1 to 0.4%, resulting from the smaller concentration or shorter lifetime of carbenium ions on the catalyst surface.

(5) Finally, we have found that the yield of secondary products decreases with increasing reaction temperature (Table 8). This too is probably due to the decrease in carbenium ion population or life time on the surface.

APPENDIX I

From the chain reaction mechanism consisting of Eqs. (2), (3), (4), (5), (6a), and (8b), we write the reaction scheme shown in detail in Table 3. In this reaction scheme, and in those for most other molecules, there are more unknown X_{0i}'s and X_{jn}'s (RPPs) than there are equations. The missing equations are not available from the type of experiment reported here and require the establishment of reaction rates for at least some of the individual carbenium ions undergoing the various reactions. This matter will be treated more fully elsewhere. Here we have adopted a

TABLE 11

Individual Rates and Activation Energies for the Reactions of 2-Methylpentane on HY

Entry no.	IRR symbol	IRR value (min^{-1})[a]			E_a[b] (kJ/mol)
		400°C	450°C	500°C	
1	r_{00}	0.038	2.56	79.40	330.8
2	r_{01}	0.106	1.48	14.67	213.2
3	r_{02}	0.038	0.49	7.77	230.2
4	r_{03}	1.121	26.20	360.74	240.7
5	r_{04}	0.826	11.52	114.78	213.4
6	r_{22}	0.023	0.49	18.12	280.9
7	r_{23}	0.674	8.87	63.86	196.8
8	r_{30}	0.235	2.86	6.04	140.5
9	r_{32}	0.053	1.48	26.75	269.2
10	r_{50}	0.045	0.49	11.22	238.3
11	r_{60}	4.325	41.27	150.20	155.1
12	r_{kc}	0.091	0.79	3.45	157.3

[a] Calculated from the equation $r_j = \mathrm{RPP}_j * \Sigma r_j$. The total reaction rate was 7.58, 98.5, and 863 min^{-1} at 400, 450, and 500°C, respectively (*22*).

[b] Calculated from the slopes of the curves in Fig. 7. These values include not only the activation energy of the corresponding rate constant but also the temperature coefficients changes in the concentration of surface species which take part in the reaction.

procedure of solving the matrix by selecting the sum of initiation reactions as the object function in a constrained solution of the set of linear equations. Furthermore, we write auxiliary equations which assume that the ratios of similar processes are equal, for example, ratios such as $X_{20}/X_{21} = X_{30}/X_{31} = X_{40}/X_{41}$. In this way we can supply all the equations necessary to obtain a unique solution.

The equations used to write the matrix a-1 come from mass balance considerations. For example propane is formed by processes subscripted as 03, 21 and 30 in Table 3. The molar selectivity for propane, P_3, is therefore equal to $X_{03} * 1 + X_{21} * 1 + X_{30} * 1$ and the coefficients (i.e., the 1's) of this equation constitute the elements of the fourth row of the matrix. Similar mass balancing applies to the production of the olefin ethylene. In that case we have to account for all the fates of ethyl carbenium ions, which are the sole source of ethylene. Thus, in this case O_2 the observed molar selectivity for ethylene comes from the difference between the total probability of production of ethyl carbenium ions and the sum of probabilities of its reaction to products other than ethylene. In that case O_2 is equal to $X_{04} * 1 - (X_{20} * 1 + X_{21} * 1 + X_{22} * 1 + X_{23} * 1)$, where the first term accounts for the formation of ethyl ions and the terms in brackets account for the reactions of these ions which do not yield ethylene. This procedure yields row 8 in the matrix.

In writing out the initiation reactions we have left out the formation of CH_3S^+. Inclusion of this reaction invariably leads to a zero value for X_{05}, the corresponding RPP. Furthermore we have included only one mode of β-cracking of $C_6H_{13}S^+$. This choice is supported by the high selectivity for propylene in the cracking of 1-hexene

(*30*) whose carbenium ion is similar to that formed here. Other β-cracking modes can be incorporated as needed. With all of this in mind, we have set up the matrix shown in (a-1) for the relationships involved in the reaction system under consideration.

$$\begin{vmatrix} 1 & 0 & 0 & 0 & 0 & 0 & 0 & 0 & 0 & 0 & 0 & 0 & 0 & 0 & 0 & 0 & 0 \\ 0 & 1 & 0 & 0 & 0 & 0 & 0 & 0 & 0 & 0 & 0 & 0 & 0 & 0 & 0 & 0 & 0 \\ 0 & 0 & 1 & 0 & 0 & 1 & 0 & 0 & 0 & 0 & 0 & 0 & 0 & 0 & 0 & 0 & 0 \\ 0 & 0 & 0 & 1 & 0 & 0 & 1 & 0 & 0 & 1 & 0 & 0 & 0 & 0 & 0 & 0 & 0 \\ 0 & 0 & 0 & 0 & 1 & 0 & 0 & 1 & 0 & 0 & 1 & 0 & 1 & 0 & 0 & 0 & 0 \\ 0 & 0 & 0 & 0 & 0 & 0 & 0 & 0 & 1 & 0 & 0 & 1 & 0 & 1 & 1 & 0 & 0 \\ 0 & 0 & 0 & 0 & 0 & 0 & 0 & 0 & 0 & 0 & 0 & 0 & 0 & 0 & 0 & 1 & 0 \\ 0 & 0 & 0 & 0 & 1 & -1 & -1 & -1 & -1 & 0 & 0 & 0 & 0 & 0 & 0 & 0 & 0 \\ 0 & 0 & 0 & 1 & 0 & 0 & 0 & 0 & 1 & -1 & -1 & -1 & 0 & 0 & 0 & 0 & 2 \\ 0 & 0 & 1 & 0 & 0 & 0 & 0 & 1 & 0 & 0 & 0 & 1 & -1 & -1 & 0 & 0 & 0 \\ 0 & 1 & 0 & 0 & 0 & 0 & 1 & 0 & 0 & 0 & 1 & 0 & 0 & 1 & -1 & 0 & 0 \\ 1 & 0 & 0 & 0 & 0 & 1 & 0 & 0 & 0 & 1 & 0 & 0 & 1 & 0 & 1 & 0 & -1 \end{vmatrix} \begin{vmatrix} X_{00} \\ X_{01} \\ X_{02} \\ X_{03} \\ X_{04} \\ X_{20} \\ X_{21} \\ X_{22} \\ X_{23} \\ X_{30} \\ X_{31} \\ X_{32} \\ X_{40} \\ X_{41} \\ X_{50} \\ X_{60} \\ X_{b63} \end{vmatrix} = \begin{vmatrix} P_H \\ P_1 \\ P_2 \\ P_3 \\ P_4 \\ P_5 \\ P_{16} \\ O_2 \\ O_3 \\ O_4 \\ O_5 \\ O_6 \end{vmatrix} \cdot \quad \text{(a-1)}$$

where P_H is the initial molar selectivity of hydrogen produced from C–H bond protolysis, as detected by experiment, P_n is the initial molar selectivity of product paraffin C_nH_{2n+2} as detected by experiment, and O_n is the initial molar selectivity of product olefin C_nH_{2n} as detected by experiment

The experimental molar selectivity values used in the solution are given in Table 1.

The coefficient matrix in (a-1) is a 12 × 17 matrix. As mentioned above we cannot obtain a unique solution in such cases from the linear relationships alone. To solve the problem, we have used the program GAMS (general algebraic modelling system) which allows the introduction of nonlinear dependencies such as the reaction probability ratios mentioned above. Both MAX and MIN of $(X_{00} + X_{01} + X_{02} + X_{03} + X_{04})$ as well as MAX X_{60} used as the object function to yield the same solution. In the case considered here for all three object functions we obtain the solution shown in Table 3. Scheme 1 is constructed using the X_{0i} and X_{jn} values from Table 3.

APPENDIX II

Further to the discussion in Appendix I, we let

03 = represent the cleavage of the C_t–C_s bond in the feed

02(or 04) = represent that of the C_s–C_s bond in the feed

01 = represent that of the C_t–C_p or C_s–C_p bond in the feed

00 = represent that of the C–H bond in the feed.

Using the results from Table 3 gives

$$BCP^{II}_{03} = \frac{X_{03}}{X_{00} + X_{01} + X_{02} + X_{03} + X_{04}} = 0.510$$

$$BCP^{II}_{02} = \frac{X_{02} + X_{04}}{X_{00} + X_{01} + X_{02} + X_{03} + X_{04}} = 0.416 \qquad \text{(a-2)}$$

$$BCP^{II}_{01} = \frac{X_{01}}{X_{00} + X_{01} + X_{02} + X_{03} + X_{04}} = 0.054$$

$$BCP^{II}_{00} = \frac{X_{00}}{X_{00} + X_{01} + X_{02} + X_{03} + X_{04}} = 0.020.$$

Scheme II has been drawn using the above data.

APPENDIX III

From Table 3 we see that propagation by $C_6H_{13}S^+$ ion leads to the formation of *i*-C_6H_{14}, its desorption leads to the production of a C_6H_{12} olefin and cracking leads to part of the total C_3H_6 olefin yield. Equation (11) may then be written

$$IC_6 = \frac{X_{60}}{O_6 + X_{b63} + X_{60}}, \qquad \text{(a-4)}$$

where O_6 is the molar selectivity for total C_6 olefin production.

Inserting the values of X_{60} from Table 3, O_6 from Table 1 and the calculated value of X_{b63} from Table 3, we have

$$IC_6 = \frac{0.5476}{0.5476 + 0.0498 + 0.0} = 0.916.$$

Other such individual ion fates can be calculated in the same way. For example the probability of a $C_4H_9^+$ ion desorbing as a product olefin is

$$OC_4 = \frac{O_4}{O_4 + X_{40} + X_{41}} = \frac{0.0170}{0.0170 + 0.0 + 0.0} = 1.0.$$

That is to say, a surface C_4^+ carbenium ion does not go on to disproportionate with a feed molecule, it simply desorbs. On the other hand,

$$OC_2 = \frac{O_2}{O_2 + X_{20} + X_{21} + X_{22} + X_{23}} = \frac{0.0203}{0.0203 + 0 + 0 + 0.005 + 0.091} = 0.175$$

indicates that ethyl ions prefer to disproportionate, while

$$OC_3 = \frac{O_3 - X_{b63}}{O_3 - X_{b63} + X_{30} + X_{31} + X_{32}} = \frac{0.1999 - 0.0}{0.1999 - 0.0 + 0.036 + 0.0 + 0.006} = 0.826$$

indicates C_3^+ carbenium ions desorb rather than take part in chain processes.

APPENDIX IV

According to the detailed description for 2-methylpentane cracking on HY zeolite given in Table 3, one can see that

$$-R_{overall} = R_{pa} + R_{coke} = (R^I_{pa} + R^P_{pa}) + R_{coke}, \qquad \text{(a-5)}$$

where $-R_{overall}$ is the feed consumption rate, R_{pa} is the sum of paraffin and molecular hydrogen formation rates (RPPs), R_{coke} is the coke formation rate (RPP), R^I_{pa} is the sum of the rate of paraffin and hydrogen formation by initiation (RPPs), and R^P_{pa} is the sum of the rate of paraffin formation by propagation (RPPs).

Compared with R^P, R^P_{pa}, or R^I_{pa}, R_{coke} is so small as to be negligible, and from Eq (14) and Table 3 we have

$$KCL = \frac{R^I_{pa} + R^P_{pa}}{R^I_{pa}}$$

$$= \frac{\Sigma_i X_{0i} + \Sigma_n \Sigma_j X_{jn}}{\Sigma_i X_{0i}} \qquad \text{(a-6)}$$

$$= \frac{0.296 + 0.694}{0.296} = 3.34.$$

A more direct, though somewhat inaccurate, method of estimating the KCL is to take

$$\text{KCL} = \frac{1 - \Sigma \text{RPP}^1}{\Sigma \text{RPP}^1 + 1}$$

$$= \frac{1 - 0.296}{0.296} + 1 = 3.38 = \frac{1}{\Sigma \text{RPP}^1}.$$

Here the first term is the number of chain events after an initiation event and 1 accounts for the conversion due to initiation. It is obvious that the minimum chain length is 1.

APPENDIX V

Assuming that the initial coke has the molecular formula C_xH_y and is formed by the pathway

$$X_{kc}C_6H_{14} \rightarrow m_k C_x H_y + m_H H_2 \qquad \text{(a-7)}$$

and that molecular hydrogen is also produced by the protolysis of a C–H bond in the feed molecule, i.e.,

$$X_{00}C_6H_{14} + X_{00}SH \rightarrow X_{00}H_2 + X_{00}C_6H_{13}S, \qquad \text{(a-8)}$$

from the reaction network presented in Table 3 we have

$$X_{00} + X_{kc} = 1 - \left(\sum_{i=1}^{4} X_{0i} + \sum_j \sum_n X_{jn}\right) \qquad \text{(a-9)}$$

$$X_{00} + m_H = S_H, \qquad \text{(a-10)}$$

where S_H is the total molar selectivity of H_2 determined by experiment.
For this mass balance in (a-7) we have

$$\begin{aligned} 6X_{kc} &= m_k x \\ 14X_{kc} &= m_k y + 2m_H. \end{aligned} \qquad \text{(a-11)}$$

For the relationship between weight and molar selectivity of coke, we have

$$S_k = F_k \frac{\text{MW}_f}{12x + y}, \qquad \text{(a-12)}$$

where S_k is the molar selectivity of coke, i.e., n_k, F_k is the weight selectivity of coke, and MW_f is the molecular weight of the feed molecule.

Using the experimental data in Table 1,

$$\begin{aligned} S_H &= 0.0172 \\ F_k &= 0.0086 \\ \text{MW}_f &= 86, \end{aligned}$$

and using the value for X_{00} from Table 3 to substitute into Eqs. (a-9) to (a-12) gives

$$\begin{aligned} m_H &= 0.0112 \\ X_{kc} &= 0.010 \\ y/x &= 1.96 \end{aligned}$$

Assuming $m_H = m_k$, gives

$$\begin{aligned} y &= 10.5 \\ x &= 5.36, \end{aligned}$$

and hence the molar weight and formula of initial coke

$$C_{5.36}H_{10.5}, \quad \text{MW} = 74.82.$$

APPENDIX VI

Quantities useful for the quantitative evaluation of a reaction mechanism:

(a) Initial weight selectivity (F_{wi}): the slope of the optimum performance envelope (wt% yield vs wt% conversion) at the origin. In all cases,

$$\sum_i F_{wi} = 1.$$

(b) Initial molar selectivity (S_{mi}):

$$S_{mi} = F_{wi}\left(\frac{\text{MW}_i}{\text{MW}_f}\right)$$

$$\Sigma S_{mi} = 1 + \varepsilon,$$

where ε is the volume expansion factor for the reaction.

(c) Reaction path probability (RPP) =

X_{0i} or X_{jn}: where i is the ith mode of protolysis, j is the number of carbons in the ion associated with the Brønsted site, and n is the number of carbons transferred to it by a gas-phase molecule. This represents the probability that the initial molecule cracked will follow the indicated path. These quantities define the reaction tendencies connected with the various paths in the network of reactions constituting the mechanism and provide the most fundamental level of quantification of the reaction mechanism.

(d) Product formation probability (PFP_i): this represents the probability of a given product appearing in the first mole of total products.

(e) Individual reaction rate (IRR_i): this is the absolute rate of a given reaction in the network of initial reactions.

$$IRR_i = X_i\left(\frac{A_1 + A_2}{1 + B}\right),$$

where

$$\left(\frac{A_1 + A_2}{1 + B}\right)$$

is the initial rate of reaction obtained from a kinetic study (*22*).

(f) Bond cleavage probability (BCP): this is the probability, relative to all modes of protolysis, that a given bond will be broken by the initial protolysis,

$$BCP_{0i}^{II} = \frac{RPP_{0i}}{\sum_{initial} RPP_{0i}},$$

where the sum in the denominator is over all reactions involving bond breaking by protolysis, i.e., reactions in path II.

APPENDIX VII: NOMENCLATURE

C_t	tertiary C
C_s	secondary C
C_p	primary C
C_6H_{14}	a feed molecule, 2-methylpentane
i-C_6H_{14}	an isomer of C_6H_{14}
SH	a Brønsted acid site
C_nH_{2n+2}	a product paraffin
$C_nH_{2n+1}S^+$	a carbenium ion associated a Brønsted site
i-$C_nH_{2n+1}S^+$	a skeletal isomer of $C_nH_{2n+1}S^+$
$C_mH_{2m-1}S^+$	a dehydrogenated precursor of coke
F	initial weight selectivity
S	initial molar selectivity
MW	molecular weight
ε	volume expansion factor
A_1, A_2, B	kinetic parameters
IRR	individual reaction rate
X_{0i}, X_{jn}	reaction path probability (RPP); see Table 3
PEP	product formation probability
BCP	bond cleavage probability
OC	olefin desorption probability
IC_6	the probability of a $C_6H_{13}S^+$ ion leading to the formation of i-C_6H_{14}
KCL	kinetic chain length
O_n	experimental selectivity for olefin C_nH_{2n}

REFERENCES

1. Pansing, W. F., *J. Phys. Chem.* **69,** 392, 1965.
2. Chen, N. Y., and Garwood, W. E., *J. Catal.* **52,** 453, 1978.
3. Weisz, P. B., *Ann. Rev. Phys. Chem.* **21,** 175, 1970.
4. McVicker, G. B., Kramer, G. M., and Ziemiak, J. J., *J. Catal.* **83,** 286, 1983.
5. Kramer, G. M., McVicker, G. B., and Ziemiak, J. J., *J. Catal.* **92,** 355, 1985.
6. Kramer, G. M., and McVicker, G. B., *J. Catal.* **115,** 608, 1989.
7. Hattori, H., Takahaski, O., Tagaki, M., and Tanabe, K., *J. Catal.* **68,** 132, 1981.
8. Hagg, W. O., and Dessau, R. M., *in* "Proceedings, 8th International Congress on Catalysis, Berlin, 1984," Vol. II, p. 305. Dechema, Berlin, 1984.
9. Corma, A., and Wojciechowski, B. W., *Catal. Rev.-Sci. Eng.* **24**(1), 1982.
10. Corma, A., Planelles, J., and Thomas, F., *J. Catal.* **93**(30), 1985.
11. Corma, A., Planelles, J., and Thomas, F., *J. Catal.* **94**(445), 1985.
12. Abbot, J., and Wojciechowski, B. W., *in* "Proceedings, 9th International Congress on Catalysis,

(M. J. Phillips and M. Ternan, Eds.), Calgary, 1988" Vol. I, p. 206. Chem. Institute of Canada, Ottawa, 1988.
13. Abbot, J., and Wojciechowski, B. W., *J. Catal.* **113,** 353, 1988.
14. Abbot, J., and Wojciechowski, B. W., *J. Catal.* **115**(1), 1989.
15. Lombardo, E. A., Pierantozzi, R., and Hall, W. K., *J. Catal.* **110**(171), 1988.
16. Lombardo, E. A., and Hall, W. K., *J. Catal.* **112**(565), 1988.
17. Hall, W. K., Lombardo, E. A., and Engelhardt, J., *J. Catal.* **115**(611), 1989.
18. Abbot, J., *Appl. Catal.* **57**(105), 1990.
19. Abbot, J., *J. Catal.* **123**(383), 1990.
20. Picket, P. E., Rabo, J. A., Dempsey, E., and Schomaker, V., *in* "Proceedings, 3rd International Congress on Catalysis," Vol. II, p. 1264. North Holland, Amsterdam, 1964.
21. Tung, S. E., and McIninch, E., *J. Catal.* **10**(166), 1968.
22. Zhao, Y. X., Bamwenda, G. R., Groten, W. A., and Wojciechowski, B. W., *J. Catal.* **140,** 243 (1993).
23. Ko, A. N., and Wojciechowski, B. W., *Prog. React. Kinet.* **12**(4), 201, 1983.
24. Wojciechowski, B. W., *Catal. Rev.-Sci. Eng.* **9**(1), 79, 1974.
25. Groten, W. A., and Wojciechowski, B. W., *J. Catal.* **122,** 362, 1990.
26. Abbot, J., and Wojciechowski, B. W., *J. Catal.* **107,** 451, 1987.
27. Wojciechowski, B. W., and Corma, A., "Catalytic Cracking," p. 31. Dekker, New York, 1986.
28. Krzywicki, A., and Marczewski, M., *J. Chem. Soc. Faraday Trans. 1* **76,** 1311, 1980.
29. Abbot, J., and Wojciechowski, B. W., *Can. J. Chem. Eng.* **66,** 825, 1988.
30. Abbot, J., and Wojciechowski, B. W., *Can. J. Chem. Eng.* **63,** 278, 1985.
31. Groten, W. A., and Wojciechowski, B. W., *J. Catal.* **140,** 262 (1993).